

See discussions, stats, and author profiles for this publication at: <https://www.researchgate.net/publication/354362867>

Multipactor Effect

Technical Report · September 2021

DOI: 10.13140/RG.2.2.22179.37924

CITATIONS

0

READS

208

1 author:



Jacques B Sombrin

Telecommunications for Space and Aeronautics

133 PUBLICATIONS 995 CITATIONS

SEE PROFILE

Some of the authors of this publication are also working on these related projects:



Behavioral modeling of high power amplifier [View project](#)



Multipactor, Corona and Passive Intermodulation [View project](#)

4 September 2021

Multipactor Effect

Jacques Sombrin

This is the English version of a CNES technical note from 10 October 1983 [12].

Table of contents

1	Introduction	3
2	Definition.....	3
3	Theory.....	3
4	Analysis	4
4.1	Secondary electrons generation	4
4.2	Trajectories of electrons	5
4.3	Limits for the phase ϕ	8
4.3.1	Electron trajectory	8
4.3.2	Envelope on the right side	10
4.4	Stability.....	11
4.5	Convergence	14
5	Study of unstable points	16
5.1	Study of modes (m, p) derived from classical modes.....	18
5.2	Analysis of modes p=2 for any value of m.....	21
5.2.1	Modes with m even.....	22
5.2.2	Modes with m odd	22
5.2.3	Limits of modes	23
6	Intermittent behavior	27
7	Comparison with experimental results	28
8	Definition of future work.....	31
8.1	Study of higher modes	31
8.2	Waveguide study	31
8.3	Numerical study.....	31
8.4	Experiments	32
9	Conclusion	32
10	Additional comments to the English version.....	32
11	Reference	33

1 Introduction

The goal of this note is to define and study multipactor effect that may be responsible of failure or even destruction of power radiofrequency equipment in vacuum, particularly satellite transmitters, output circuits and antennas. The knowledge of the conditions for multipactor effect is essential for satellite design, particularly those transmitting high power such as direct television and synthetic aperture radars (SAR). This study has been done in part to support EOPO (Earth Observation Program Office) for the SAR satellite ERS1.

The theoretical study is based on previous simple and empirical studies. It shows the limitations of these theories and of the classical definition of multipactor effect. A more rigorous analytical study is proposed. By applying simple physical criteria (stability or instability, limit conditions, ...) more interesting results are obtained without requiring empirical values.

Then, after comparing theoretical results with published or obtained experimental results, this note proposes directions for further work and a better knowledge of the phenomenon.

2 Definition

Multipactor effect is an electron avalanche (exponential increase of the number of electrons versus time) phenomenon that happens in certain resonance conditions and in vacuum (less than 0.1 mm Hg):

- A voltage $V = V_0 \sin(2\pi ft)$ is applied between two plates at a distance d ,
- Free mean path of electrons $\gg d$
- If an electron starts from one plate at a given phase ϕ (or time $\frac{\phi}{\pi f}$) and is accelerated to the other plate in a duration $(2n - 1)T/2$ with $T = 1/f$,
- If the speed of the electron is high enough to generate more than one secondary electron on this second plate,
- Then these secondary electrons will be accelerated again toward the first plate in $(2n - 1)T/2$ and the phenomenon will repeat with an increase of the number of electrons at each cycle.

The resulting electron flux may erode metallic surfaces, generate RF noise, detune cavities resonant frequency and, in some cases, create outgassing that will in turn induce a voltage breakdown and a possible destruction of the equipment [1].

3 Theory

The simplest theory that describes multipactor effect between two parallel plates is given by Hatch and Williams [2, 3]. The main hypothesis in this theory is that the final speed of electrons participating in the avalanche is proportional to the initial speed of these electrons. The initial speed of secondary electrons is experimentally known not to be influenced by the speed of primary electrons. One must suppose that the multipactor effect "makes some choice" in available secondary electrons.

This simple theory uses some experimental values to limit the phases that can generate multipactor effect.

It seems to be difficult to generalize this theory to more complex geometries, such as irises in waveguide filters and slots in waveguide antennas.

Another theory considers that the initial speed is constant (equal to the most probable secondary electrons speed).

It is then possible to study the distribution of phases of electrons versus the distribution of secondary electrons speeds and the number of generated secondary electrons versus the speed of primary electrons. This is simulated on a computer [4].

In this paper, we study this theory, using as much analysis as possible before numerical computation. Particularly, we will deduct physical limits for useful phases of electros. We will also demonstrate the bunching of electrons participating to the effect.

4 Analysis

4.1 Secondary electrons generation

Let us consider the two following curves from [5]:

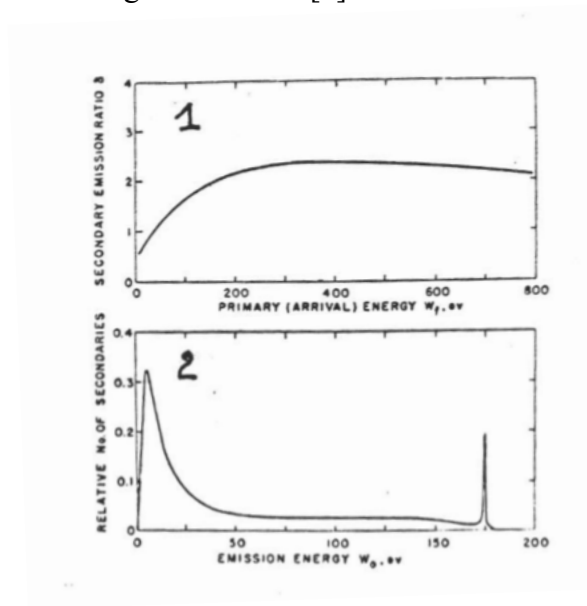


Figure 1 and 2 from [5]

Figure 1 is the number of secondary electrons generated versus energy of primary electrons. This curve is flat, and the number of secondary electrons may be higher than one between two values of final energy of the primary electron:

$$18 \text{ eV} < eW_{fmin} < 50 \text{ eV}$$

$$2\,000 \text{ eV} < eW_{fmax} < 10\,000 \text{ eV}$$

If the ratio of secondary electrons to primary electrons is always lower than 1 , no multipactor effect can occur.

Figure 2 is the number of secondary electrons versus their emission energy. This curve has a sharp peak corresponding to the most probable energy and a speed of:

$$eW_i = \text{some eV}$$

We will generally use the values proposed in [1]: $eW_{fmin} = 18 \text{ eV}$ and $eW_i = 5 \text{ eV}$.

We will use maximum values eW_{fmax} up to 18 000 eV.

4.2 Trajectories of electrons

The electromagnetic field is created by the voltage $V = V_0 \sin(\omega t)$ between two plates at abscissas $x = 0$ and $x = d$.

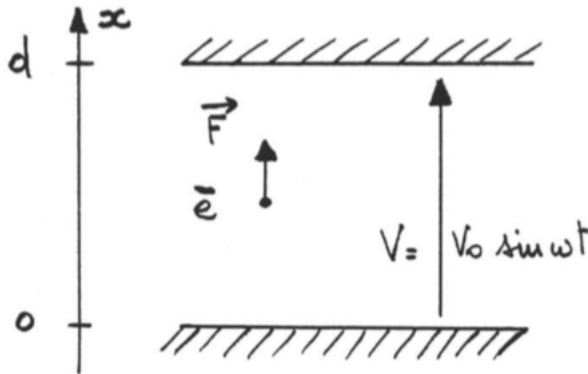


Figure 3

The electric field is: $E = \frac{-V_0}{d} \sin(\omega t)$

The force applied to the electron with charge $-e$ is: $F = -eE = e \frac{V_0}{d} \sin(\omega t)$

Note that:

$$\omega = 2\pi f$$

$$e = 1,59 \cdot 10^{-19} \text{ Coulomb}$$

$$m = 9,035 \cdot 10^{-31} \text{ kg}$$

$$e/m = 0,17598 \cdot 10^{12} \text{ C/kg}$$

The relation between speed and energy is: $eW = \frac{1}{2} m v^2$.

The electron acceleration is:

$$\ddot{x}(t) = \frac{e V_0}{m d} \sin(\omega t)$$

By integrating this equation and supposing that the initial speed is v_i at time $t_i = \phi/\omega$:

$$\dot{x}(t) = v_i - \frac{e V_0}{m \omega d} [\cos(\omega t) - \cos \phi]$$

By integrating a second time with $x=0$ at initial time:

$$x(t) = v_i(t - t_i) - \frac{e V_0}{m \omega d} \left\{ \frac{1}{\omega} [\sin(\omega t) - \sin \phi] - (t - t_i) \cos \phi \right\}$$

By using $\theta = \omega t$, we get:

$$\ddot{x}(\theta) = \frac{e V_0}{m d} \sin \theta$$

$$\dot{x}(\theta) = v_i - \frac{e V_0}{m \omega d} [\cos \theta - \cos \phi]$$

$$\omega x(\theta) = v_i(\theta - \phi) - \frac{e V_0}{m \omega d} \{ \sin \theta - \sin \phi - (\theta - \phi) \cos \phi \}$$

Let us now consider the final time:

$$t_f = t_i + \frac{(2n-1)T}{2} = t_i + \frac{(2n-1)}{2f} = t_i + \frac{(2n-1)\pi}{\omega}$$

That is the phase $\theta_f = \phi + (2n+1)\pi$.

We get:

$$\ddot{x}(\theta_f) = \frac{e V_0}{m d} \sin \theta_f = \frac{e V_0}{m d} \sin \phi$$

$$\dot{x}(\theta_f) = v_i + \frac{e V_0}{m \omega d} \cos \phi$$

$$\omega x(\theta_f) = v_i(2n-1)\pi + \frac{e V_0}{m \omega d} \{2 \sin \phi + (2n-1)\pi \cos \phi\}$$

We can see that 3 conditions are necessary for multipactor effect to occur:

1) The position $x(\theta_f)$ must be equal to d :

$$\omega d = v_i(2n-1)\pi + \frac{e V_0}{m \omega d} \{2 \sin \phi + (2n-1)\pi \cos \phi\}$$

$$\frac{\omega d}{e/m} [\omega d - v_i(2n-1)\pi] = V_0 \{2 \sin \phi + (2n-1)\pi \cos \phi\}$$

2) The final speed must be greater or equal to $v_{f \min}$ with $eW_{f \min} = \frac{1}{2} m v_{f \min}^2$ or:

$$\frac{\omega d}{e/m} (v_{f \min} - v_i) \leq 2V_0 \cos \phi$$

3) The final speed must be smaller or equal to $v_{f \max}$ with $eW_{f \max} = \frac{1}{2} m v_{f \max}^2$ or:

$$\frac{\omega d}{e/m} (v_{f \max} - v_i) \geq 2V_0 \cos \phi$$

In fact, we can choose the final speed $\dot{x}(\theta_f) = v_f$ with $v_{f \min} \leq v_f \leq v_{f \max}$ so that:

$$\frac{\omega d}{e/m} (v_f - v_i) = 2V_0 \cos \phi$$

The two equalities give relations between V_0 , ωd and v_f at $v_i = \text{constant}$:

$$\frac{\omega d}{e/m} [\omega d - v_i(2n-1)\pi] = V_0 \{2 \sin \phi + (2n-1)\pi \cos \phi\}$$

And

$$\frac{\omega d}{e/m} (v_f - v_i) = 2V_0 \cos \phi$$

From these we get:

$$\frac{\omega d}{e/m} \left[\omega d - \frac{(2n-1)\pi}{2} (v_f + v_i) \right] = 2V_0 \sin \phi$$

Then:

$$\tan \phi = \frac{\omega d - \frac{(2n-1)\pi}{2} (v_f + v_i)}{v_f - v_i}$$

As $\omega d \geq 0$ and $v_f \geq v_i$, then

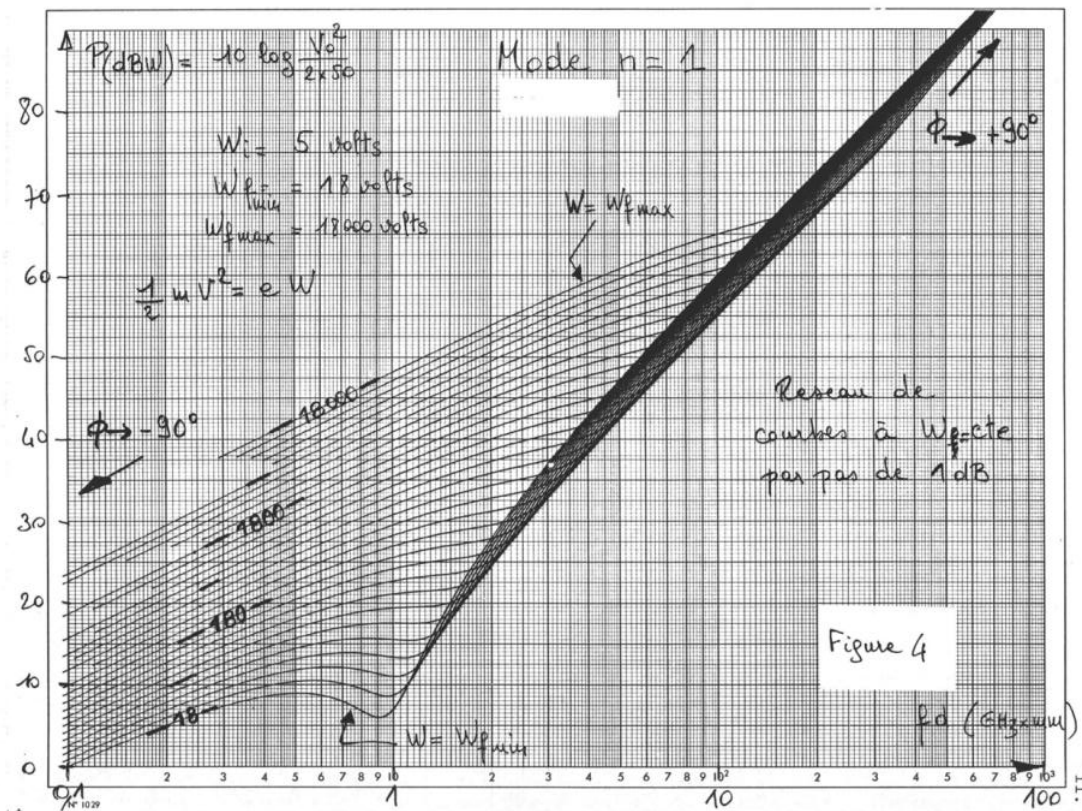
$$\tan \phi \geq -\frac{(2n-1)\pi}{2} \frac{(v_f + v_i)}{v_f - v_i}$$

Using $\cos^2 \phi = \frac{1}{1 + \tan^2 \phi}$:

$$V_0 = \frac{\omega d (v_f - v_i)}{2 e/m \cos \phi} = \frac{\omega d (v_f - v_i)}{2 e/m} \sqrt{1 + \tan^2 \phi}$$

$$V_0 = \frac{\omega d (v_f - v_i)}{2 e/m} \sqrt{(v_f - v_i)^2 + \left[\omega d - \frac{(2n-1)\pi}{2} (v_f + v_i) \right]^2}$$

We can plot a set of curves of V_0 versus ωd or fd for values of the parameter v_f from $v_{f \min}$ to $v_{f \max}$. We use logarithmic coordinates. Along each curve, the phase ϕ varies from -90° to $+90^\circ$. See figure 4 for $n = 1$.



We can plot such a set of curves for each mode given by an integer parameter n (or the mode given by the odd integer $2n - 1$).

The minimum curves in each set have a minimum envelope given by a straight line:

$$V_0 = \frac{\omega d (v_{f \min} - v_i)}{2 e/m}$$

Each minimum curve is tangent to the minimum envelope at points where $\phi = 0$ and

$$\omega d = \frac{(2n - 1)\pi}{2} (v_{f \min} + v_i)$$

In logarithmic coordinates the envelope equation gives the power (in dBW) in a 50 ohms load versus the frequency distance product fd (in GHz x mm) as:

$$P(\text{dBW}) = 10 \log \left(\frac{V_0^2}{2Z_0} \right) = 20 \log \left(2\pi \frac{v_{f \min} - v_i}{20 e/m} \right) + 20 \log(fd)$$

Or:

$$P(\text{dBW}) = 6.55 + 20 \log(fd)$$

4.3 Limits for the phase ϕ

The three necessary conditions are not sufficient for multipactor effect to occur. Other conditions must be added. They will limit the values of phases ϕ for each of the curves that have been obtained.

4.3.1 Electron trajectory

The first condition is that the electron trajectory must not go through positions less than 0 or higher than d before the final time t_f or phase $\theta_f = \omega t_f$.

We compute for the first case. The other one can be computed in the same way, but it is always verified and does not limit the initial phase.

We compute the minimum phase ϕ_{\min} that gives $x = 0$ and $\dot{x} = 0$ at some time t_0 or phase $\theta_0 = \omega t_0$. Under this limit value ϕ_{\min} the electron trajectory will go under $x = 0$ as seen in figure 5.

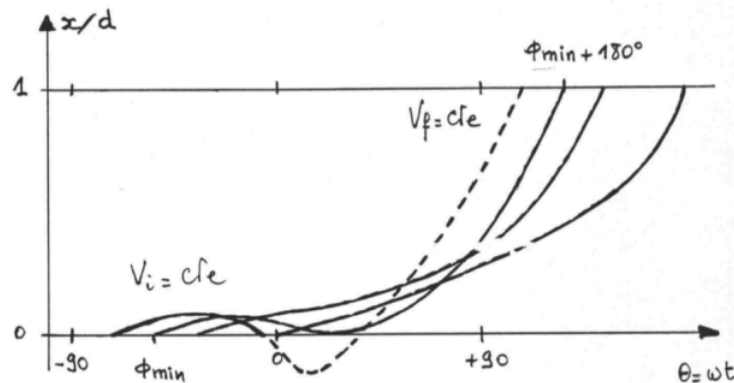


Figure 5

We have the following relation $\dot{x}(\theta_0) = 0$ and

$$\dot{x}(\theta_0) = v_i - \frac{e V_0}{m \omega d} [\cos \theta_0 - \cos \phi_{min}] = 0$$

So that:

$$\cos \theta_0 = \cos \phi_{min} + \frac{v_i \omega d}{V_0 e/m}$$

As the final speed is v_f (when limit trajectory goes to $x = d$), we have also:

$$\cos \phi_{min} = \frac{(v_f - v_i) \omega d}{2 V_0 e/m}$$

Then we have:

$$\cos \theta_0 = \frac{(v_f + v_i) \omega d}{2 V_0 e/m}$$

This phase θ_0 exists only if $\frac{(v_f + v_i) \omega d}{2 V_0 e/m} \leq 1$.

The value of x at phase θ_0 is such that:

$$\omega x(\theta_0) = v_i(\theta_0 - \phi_{min}) - \frac{e V_0}{m \omega d} \{ \sin \theta_0 - \sin \phi_{min} - (\theta_0 - \phi_{min}) \cos \phi_{min} \}$$

$$\omega x(\theta_0) = \frac{e V_0}{m \omega d} \left\{ (\theta_0 - \phi_{min}) \left(\frac{v_i \omega d}{V_0 e/m} + \cos \phi_{min} \right) - \sin \theta_0 + \sin \phi_{min} \right\}$$

$$\omega x(\theta_0) = \frac{e V_0}{m \omega d} \{ (\theta_0 - \phi_{min}) \cos \theta_0 - \sin \theta_0 + \sin \phi_{min} \}$$

Note that $|\theta_0| \leq |\phi_{min}|$ as $\cos \theta_0 \geq \cos \phi_{min}$.

Interesting solutions are given by $\theta_0 > \phi_{min}$ or $t_0 > t_{min}$.

So, we look for a solution with:

$$\cos \phi_{min} = \frac{(v_f - v_i) \omega d}{2 V_0 e/m} \quad \text{and} \quad \phi_{min} < 0$$

$$\cos \theta_0 = \frac{(v_f + v_i) \omega d}{2 V_0 e/m} \quad \text{and} \quad \theta_0 > 0$$

$$(\theta_0 - \phi_{min}) \cos \theta_0 - \sin \theta_0 + \sin \phi_{min} = 0.$$

Using $X = \frac{f d}{V_0}$, $\alpha = \frac{\pi(v_f + v_i)}{e/m}$, and $\beta = \frac{\pi(v_f - v_i)}{e/m}$, we get:

$$(a \cos \alpha X + a \cos \beta X) X - \sqrt{1 - \alpha^2 X^2} - \sqrt{1 - \beta^2 X^2} = 0$$

After numerical resolution for X we get:

$$\phi_{min} = -a \cos \beta X$$

The phase ϕ_{min} depend only on v_f and v_i and not on parameter n or mode $2n - 1$.

Values go from -64° for $eW_{fmin} = 18 \text{ eV}$ to -16.9° for $eW_{fmax} = 18\,000 \text{ eV}$.

4.3.2 Envelope on the right side

The second condition is obtained following the remark that the set of curves in figure 4 are folded on themselves and that two curves go through some points in the graph.

The set has an envelope on the side $fd \nearrow, V_0 \searrow$.

The equation of this envelope can be obtained by computing the lowest voltage V_0 that may sustain multipactor effect at a given value of fd and parameter n .

From the equation:

$$\frac{\omega d}{e/m} [\omega d - v_i(2n - 1)\pi] = V_0 \{2 \sin \phi + (2n - 1) \pi \cos \phi\}$$

The minimum voltage V_{0min} is obtained when $2 \sin \phi + (2n - 1) \pi \cos \phi$ is maximum.

The derivative versus phase ϕ is 0 for ϕ_{max} :

$$2 \cos \phi_{max} - (2n - 1) \pi \sin \phi_{max}$$

Then:

$$\tan \phi_{max} = \frac{2}{(2n - 1) \pi}$$

The maximum phase depends on the mode:

$$\begin{aligned} \phi_{max} &= 32.48^\circ & \text{for } n=1 \\ \phi_{max} &= 11.98^\circ & \text{for } n=2 \\ \phi_{max} &= 7.26^\circ & \text{for } n=3 \dots \end{aligned}$$

The corresponding final speed is obtained from equation:

$$\tan \phi_{max} = \frac{\omega d - (v_f + v_i)(2n - 1)\pi/2}{v_f - v_i} = \frac{2}{(2n - 1) \pi}$$

That is:

$$v_f = \frac{2\pi(2n - 1) \omega d + [4 - (2n + 1)^2\pi^2]v_i}{4 + (2n - 1)^2\pi^2}$$

We also get the minimum voltage:

$$V_{0min} = \frac{\omega d [\omega d - v_i(2n - 1)\pi]}{e/m \sqrt{4 - (2n + 1)^2\pi^2}}$$

When the phase is higher than this maximum, the curve corresponding to a given final speed v_f folds back on the inside of the set of curves after being tangential to the envelope. This curve crosses curves corresponding to higher values of final speed. In a part of the (V_0, fd) plane, at each point, there are two curves with different final speeds and the point corresponds to two different phases, one for each curve.

One question is about the stability of multipactor effect at this point and to determine which part of the curves and which set of parameters (v_f, ϕ) gives a stable effect (or both or none).

4.4 Stability

The multipactor effect will be said to be stable if a small variation of initial phase ϕ will tend to decrease as a function of time.

We start from a nominal position given by parameters v_i , fd and V_0 .

The electron trajectory is:

$$\omega x(\theta) = v_i(\theta - \phi) - \frac{e V_0}{m \omega d} \{ \sin \theta - \sin \phi - (\theta - \phi) \cos \phi \}$$

We study this trajectory for initial phase values that are near the nominal value ϕ that result in $x = d$ and $\dot{x} = v_f$ at $\theta = \phi + (2n - 1)\pi$:

$$\omega x(\phi + (2n - 1)\pi) = v_i(2n - 1)\pi + \frac{e V_0}{m \omega d} \{ 2 \sin \phi + (2n - 1)\pi \cos \phi \}$$

The derivative with respect to the initial phase is:

$$\frac{\partial \omega x}{\partial \phi} = \frac{e V_0}{m \omega d} \{ 2 \cos \phi - (2n - 1)\pi \sin \phi \}$$

Nota: sign error in original manuscript corrected.

A small variation of initial phase $d\phi_1$ will result in a variation of position $(2n - 1)$ half periods later at phase $\theta + d\phi_1 = \phi + d\phi_1 + (2n - 1)\pi$:

$$d(\omega x) = \frac{e V_0}{m \omega d} \{ 2 \cos \phi - (2n - 1)\pi \sin \phi \} d\phi_1$$

From the final speed, approximately v_f we derive the phase $\theta + d\theta + d\phi_1$ at which the electron reaches $x = d$: $d\theta = -\omega dt = -\omega \frac{dx}{v_f} = -\frac{d(\omega x)}{v_f}$.

That is:

$$d\theta = -\frac{1}{v_f} \frac{e V_0}{m \omega d} \{ 2 \cos \phi - (2n - 1)\pi \sin \phi \} d\phi_1$$

The final phase is:

$$\theta + d\theta + d\phi_1 = \phi + d\theta + d\phi_1 + (2n - 1)\pi$$

The phase delay is:

$$d\theta + d\phi_1 = \left[1 - \frac{1}{v_f} \frac{e V_0}{m \omega d} \{ 2 \cos \phi - (2n - 1)\pi \sin \phi \} \right] d\phi_1$$

The phase is stable if and only if:

$$-1 \leq 1 - \frac{1}{v_f} \frac{e V_0}{m \omega d} \{ 2 \cos \phi - (2n - 1)\pi \sin \phi \} \leq 1$$

We get two limits for phase stability:

$$1) \quad \frac{1}{v_f} \frac{e V_0}{m \omega d} \{ 2 \cos \phi - (2n - 1)\pi \sin \phi \} \geq 0$$

Or: $\phi \leq \phi_{max}$ with $\tan \phi_{max} = \frac{2}{(2n-1)\pi}$

This value is identical to the phase obtained through the computation of the envelope of the set of curves. We conclude that the part of each curve with $\phi > \phi_{max}$ is not stable and does not contribute to sustained multipactor effect and that on each point in the (V_0, fd) plane there is only one curve and one set of parameters (v_f, ϕ) that results in multipactor effect.

2) $\frac{1}{v_f} \frac{e}{m} \frac{V_0}{\omega d} \{2 \cos \phi - (2n - 1)\pi \sin \phi\} \leq 2$

Or: $2 \cos \phi - (2n - 1)\pi \sin \phi \leq \frac{2v_f \omega d}{e/m V_0} = \frac{4v_f \cos \phi}{v_f - v_i}$

$$2 \cos \phi \left(1 - \frac{2v_f}{v_f - v_i}\right) \leq (2n - 1)\pi \sin \phi$$

$$\tan \phi \geq \frac{-2(v_f + v_i)}{(2n - 1)\pi(v_f - v_i)}$$

We get the condition $\phi \geq \phi_{min}$ with:

$$\tan \phi_{min} = \frac{-2(v_f + v_i)}{(2n - 1)\pi(v_f - v_i)}$$

This stability minimum phase limit is different from the one obtained with the equation in X for trajectories not being negative. Both conditions must be respected.

However, we can see that the equation in X will give a value $\phi_{min X}$ higher than the one for stability only for $n = 1$ and for high values of v_f .

For all other modes the stability condition is sufficient.

Starting with this limit phase in the equation:

$$\tan \phi = \frac{\omega d - \frac{(2n - 1)\pi}{2}(v_f + v_i)}{v_f - v_i}$$

We get:

$$\omega d - \frac{(2n - 1)\pi}{2}(v_f + v_i) = \frac{-2(v_f + v_i)}{(2n - 1)\pi}$$

$$\omega d = \frac{(2n - 1)^2 \pi^2 - 4}{2(2n - 1)\pi}(v_f + v_i)$$

$$f d = \frac{(2n - 1)^2 \pi^2 - 4}{4(2n - 1)\pi^2}(v_f + v_i)$$

For the minimum speed $v_{f min}$, we get the minimum value of the frequency distance product to sustain multipactor:

$$fd_{min} = \frac{(2n - 1)^2 \pi^2 - 4}{4 (2n - 1) \pi^2} (v_{f min} + v_i)$$

For the first mode $n=1$ and parameters $eW_i = 5 eV$ and $eW_{fmin} = 18 eV$, we get the cut-off for frequency-distance product:

$$fd_{min} = 0.57 \text{ GHz} \cdot \text{mm}$$

Remark that $|\phi_{min}|$ decreases when the mode number $(2n - 1)$ increases.

Higher modes are reduced to very thin stability domains, see figure 6.

These domains are much larger if stability is not accounted for, see figure 7.

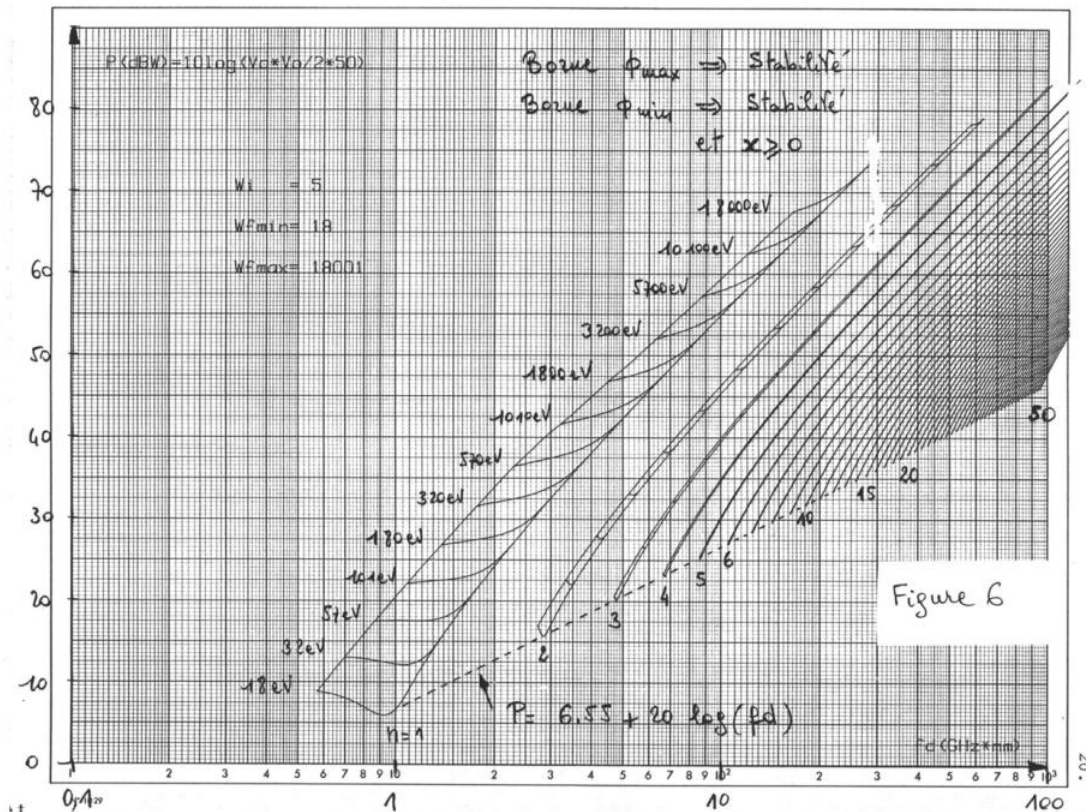
The stability criterion also proves that:

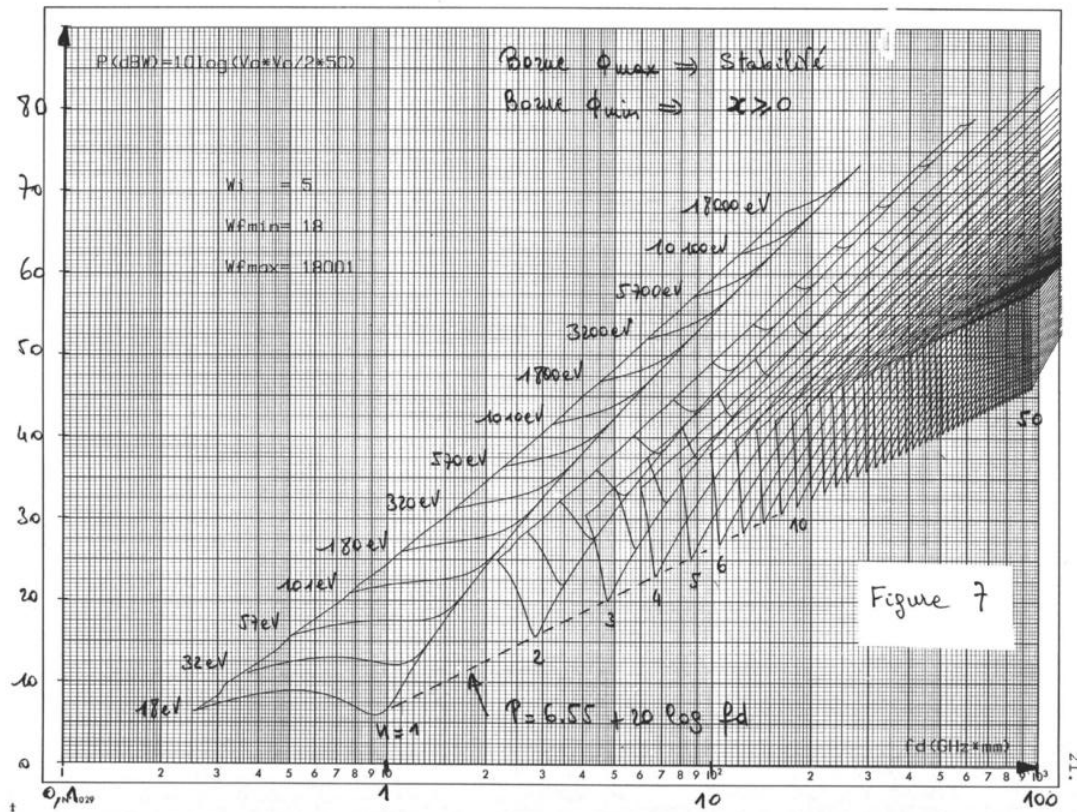
- 1) higher modes do not mingle (at constant initial speed value v_i)
- 2) electrons participating in the multipactor effect tend to bunch around the stable phase for given parameters v_i , fd and V_0 .

The maximum stability is given by: $\frac{d\theta+d\phi}{d\phi} = 0$.

Or: $\frac{1}{v_f} \frac{e}{m} \frac{V_0}{\omega d} \{2 \cos \phi - (2n - 1)\pi \sin \phi\} = 1$.

The most stable initial phase is: $\tan \phi_{stab} \geq \frac{-(v_f+v_i)}{(2n-1)\pi(v_f-v_i)}$.





4.5 Convergence

For given parameters v_i , fd and V_0 at most one initial phase exists that gives a stable multipactor effect. Around this phase, a range of convergence $[\phi_1, \phi_2]$ can be defined such that any electron with an initial phase inside this range will converge to an initial phase ϕ_0 and electrons with an initial phase outside this range will diverge and no longer participate to the multipactor effect, meaning that after a certain time their final speed will be outside the range $[v_{f \min}, v_{f \max}]$ giving a yield higher than 1.

A FORTRAN program has been written to study this convergence. The trajectory of one electron with parameters v_i , fd and V_0 is followed for time steps corresponding to 1° phase steps. When the position x becomes higher than d , a linear interpolation gives the time at which the electron strikes the $x = d$ plate.

At this time and position, the speed is computed and if it is in the range $[v_{f \min}, v_{f \max}]$, the secondary electron trajectory is followed with initial speed $-v_i$ and initial position d .

At each cycle, the initial and final phases and the final speed are printed.

In a first implementation, the linear interpolation was not computed, and the final phase was known with up to 0.5° quantification error.

This quantification error is not acceptable because it can stabilize some instable points of the curves. If the divergence is less than 0.5° at each trajectory, it is brought back to 0° .

With the implementation of linear interpolation, no unwanted stabilization has been obtained, at least for small order modes where it is possible to verify by analysis.

This shows the possible difficulties in going directly to a numerical analysis as a function of initial speed distribution.

Particularly, results in [4] are obtained with a code that bunches electrons initial phases by ranges of 5° . It is quite possible that some effects related in this paper come from this computation method (strong convergence for negative phases).

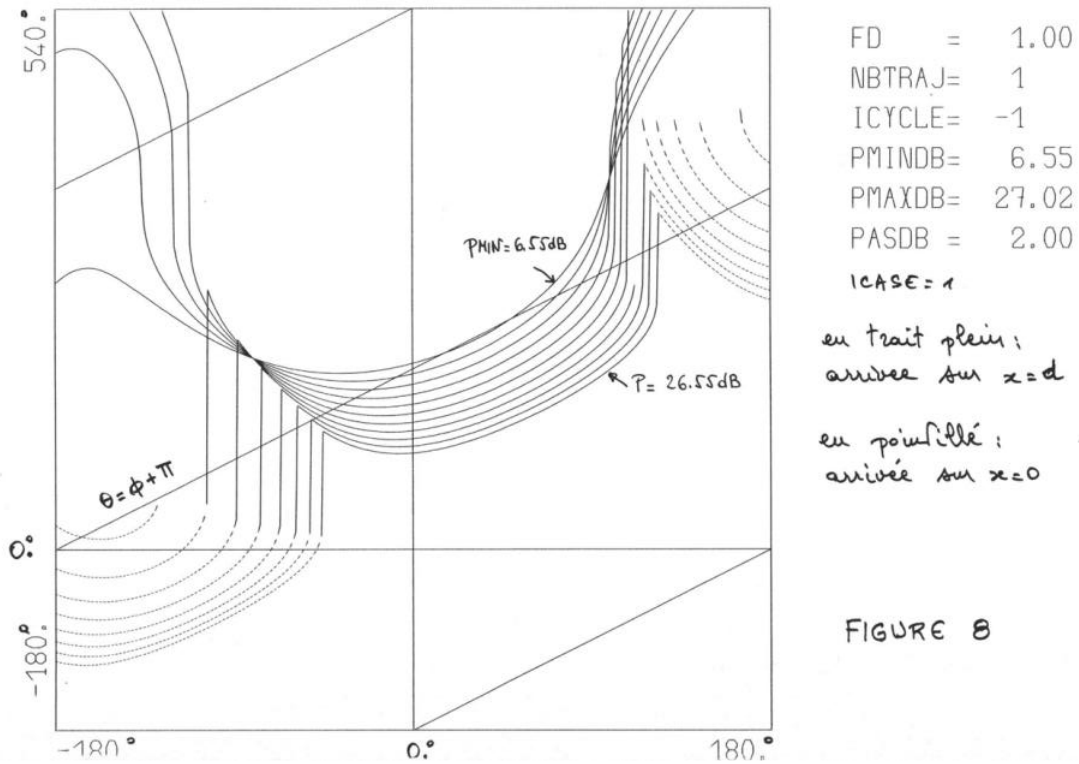
This explains why we use a lengthy theoretical analysis before numerical analysis.

Figure 8 shows the final phase of an electron versus its initial phase or $fd = 1 \text{ GHz} \times \text{mm}$ and for different values of voltage V_0 .

Figure 9 shows the same curves but limited to final speeds in the range $[v_{f \text{ min}}, v_{f \text{ max}}]$ giving more secondary electrons than primary electrons.

Convergence towards stable phases happens in a range that may reach 180° for the highest voltages.

It can be seen also that for phases between 90° and 180° , (dashed lines), the primary electron goes back to the initial plate at $x = 0$ with a speed $v_f \geq v_{f \text{ min}}$.



$$\theta_2 = \theta'_2 + \pi = \theta_f(\phi_2 - \pi) + \pi = \phi_1 + 2\pi$$

Leading to:

$$\theta_2 = \theta_f^-(\phi_2) = \phi_1 + 2\pi$$

After two trajectories from one plate to the other one, the electron gets back to plate $x = 0$ with a phase increased by 2π . The avalanche effect can go on and the number of electrons can augment if the final speed is in the range giving higher than 1 yield.

In the same manner, if $\phi'_1 = \phi_1 + \pi$, we get:

$$\theta'_2 = \theta_f(\phi'_2) = \phi'_1$$

And

$$\theta'_1 = \theta_f^-(\phi'_1) = \phi'_2 + 2\pi$$

Electrons travel as two planes instead of plane as in the classical definition. An example is given in figure 11.

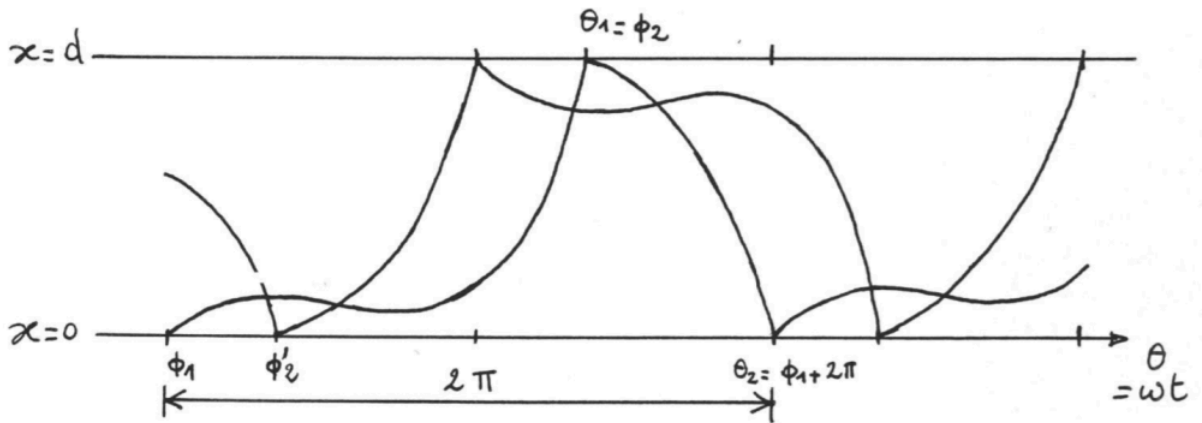


FIGURE 11

Classical multipactor modes are cases of cycles of p trajectories between plates where the electron comes back to the first plate with a phase increased by $2m\pi$.

The classical modes given by $p = 2$ and $m = 2n - 1$ with the additional condition that the movement is alternate and symmetrical between the two plates.

5.1 Study of modes (m, p) derived from classical modes

In general [7], the existence of a stable mode is sufficient to demonstrate that the derivatives $\frac{d\theta_2}{d\phi_1}$ and $\frac{d\theta_1}{d\phi_2}$ are equals. We have:

$$\frac{d\theta_2}{d\phi_1} = \frac{d\theta'_2}{d\phi_1} = \frac{d\theta'_2}{d\phi'_2} \cdot \frac{d\phi'_2}{d\phi_1} = \theta'_f(\phi'_2) \cdot \theta'_f(\phi_1)$$

And

$$\frac{d\theta_1}{d\phi_2} = \frac{d\theta_1}{d\phi'_2} = \frac{d\theta_1}{d\phi_1} \cdot \frac{d\phi_1}{d\phi'_2} = \theta'_f(\phi_1) \cdot \theta'_f(\phi'_2)$$

These two derivatives are equal to the product of the two derivatives at the corners of the stable cycle.

This cycle is stable if the derivative is between -1 and +1. If we increase again the voltage V_0 , this value decreases under -1. The two-phase (ϕ_1, ϕ'_2) cycle is no longer stable. In fact, each point gives two new points, and we get a 4-phase cycle that is stable. When increasing the voltage V_0 , and for smaller and smaller increments, we get longer and longer cycles with $p = 2^q$ trajectories between plates.

Generally, there is a critical value for the driving parameter for this doubling of cycles (for us V_0) after which the cycle becomes infinite and successive phases seem to be random.

A slight modification of initial phase result in a completely different trajectory. The movement becomes turbulent, it is no longer laminar.

With the experimental values that we use, ($eW_i = 5 eV$ and $eW_{fmin} = 18 eV$), the first mode, $m = 1$ and $p = 2$ is limited by the condition $x > 0$ and not by stability. There are no cycles with more than 2 phases. The mode $m=3$, a generalization of mode $n = 1$ ($2n - 1 = 1$) gives cycles with 4 and 8 phases at least. Higher modes may allow turbulent cycles. However, each of these modes is thin and the widening of the corresponding mode may be low.

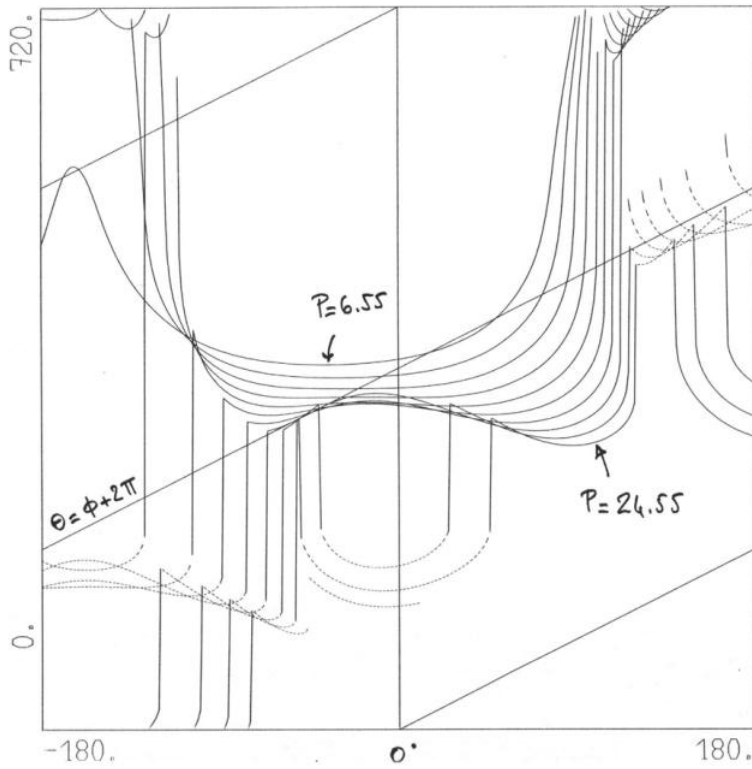
The widening of the first mode ($m = 1, p = 2$) is quite visible and the curves for the phases have been studied:

$$\theta = \theta_f^- [\theta_f(\phi)] \quad \text{if the end of the first step is on } x = d.$$

$$\theta = \theta_f [\theta_f(\phi)] \quad \text{if the end of the first step is on } x = 0.$$

These curves are given in figure 12 for all trajectories and in figure 13 for trajectories with final speed higher than v_{fmin} with a zoom in figure 14.

In this last figure, phases ϕ_1 and ϕ'_2 of figure 10 are now stable for this 2-cycle.

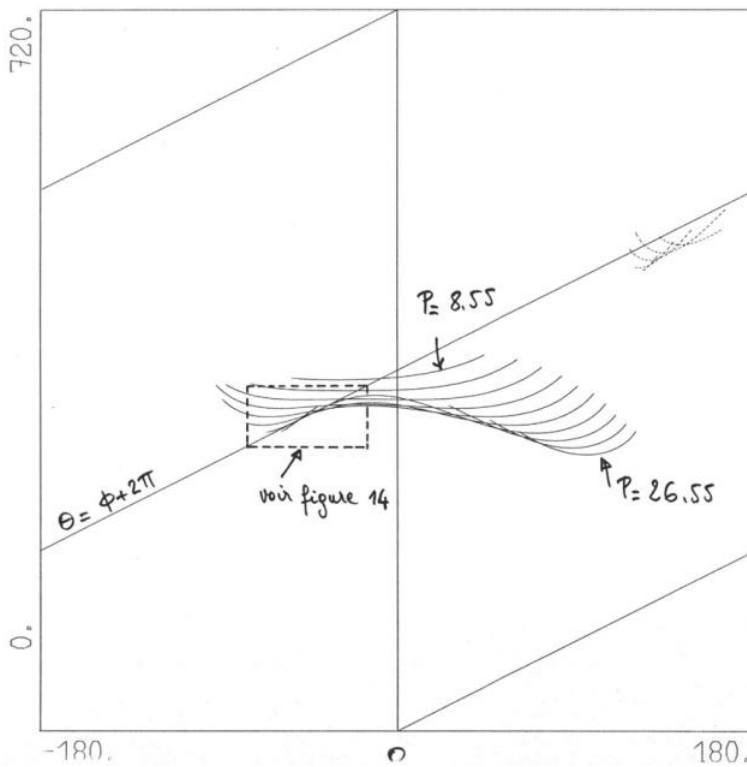


FD = 1.00
 NBTRAJ= 2
 ICYCLE= 1
 PMINDB= 6.55
 PMAXDB= 27.02
 PASDB = 2.00
 ICASE = 1

en trait plein :
 arrivée sur $x=0$
 en pointillé :
 arrivée sur $x=d$

FIGURE 12

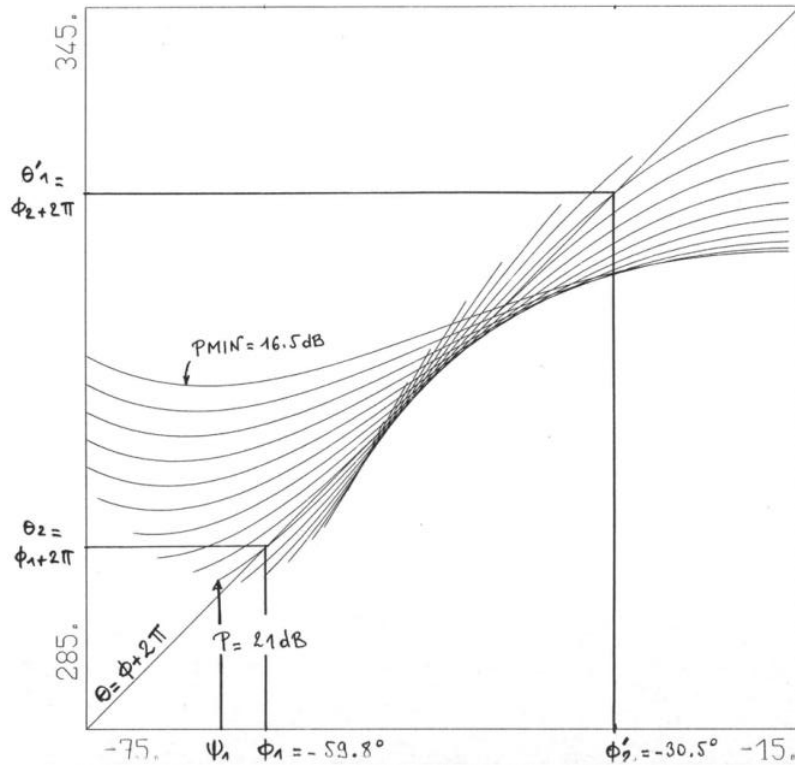
32.



FD = 1.00
 NBTRAJ= 2
 ICYCLE= 1
 ICASE = 2
 PMINDB= 6.55
 PMAXDB= 27.02
 PASDB = 2.00

FIGURE 13

33.



FD = 1.00
 NBTRAJ= 2
 ICYCLE= 1
 ICASE = 2
 PMINDB= 16.50
 PMAxDB= 26.55
 PASDB = .50

ϕ_1 et ϕ_2 points
 stables après
 2 trajets
 ψ_1 limite de convergence
 vers ϕ_1

FIGURE 14

5.2 Analysis of modes $p=2$ for any value of m

These modes are the simplest ones after the classically defined modes. The mode $p = 2$, $m = 1$ is the generalization of the classical first mode $n = 1$, $m = 2n - 1 = 1$.

The mode $p = 2$, $m = 3$ is a generalization of the next classical mode $n = 2$, $m = 2n - 1 = 3$.

However, the mode $p = 2$, $m = 2$ (and modes $p = 2$, $m = 2q$) are new.

We study movements that alternate between the two plates but are not necessarily symmetrical:

From $x = 0$ to $x = d$; phase from ϕ_1 to $\theta_1 = \theta_f(\phi_1)$

From $x = d$ to $x = 0$; phase from $\phi_2 = \theta_1$ to $\theta_2 = \theta_f^-(\phi_2)$

With $\phi_2 = \phi_1 + 2m\pi$

Function θ_f^- is obtained by changing the sign of voltage V_0 and so of the parameter β .

The following relations are obtained:

$$1 = [\sqrt{2\gamma} + \beta \cos \phi_1](\phi_2 - \phi_1) - \beta[\sin \phi_2 - \sin \phi_1]$$

$$\frac{v_{f1}}{\omega d} = \beta(\cos \phi_1 - \cos \phi_2) + \sqrt{2\gamma}$$

And:

$$1 = [\sqrt{2\gamma} - \beta \cos \phi_2](\phi_1 + 2m\pi - \phi_2) + \beta[\sin \phi_1 - \sin \phi_2]$$

$$\frac{v_{f2}}{\omega d} = -\beta(\cos \phi_2 - \cos \phi_1) + \sqrt{2\gamma}$$

We can see that both final speeds are equals even if the trajectories are not symmetrical.

$$\frac{v_f}{\omega d} = \beta(\cos \phi_1 - \cos \phi_2) + \sqrt{2\gamma}$$

Let us define: $\phi'_2 = \phi_2 - m \pi$ and examine case with m either even or odd.

5.2.1 Modes with m even

If m is even, we have the 3 following relations:

$$1 = [\sqrt{2\gamma} + \beta \cos \phi_1](\phi'_2 - \phi_1 + m \pi) - \beta[\sin \phi'_2 - \sin \phi_1]$$

$$1 = [-\sqrt{2\gamma} + \beta \cos \phi'_2](\phi'_2 - \phi_1 - m \pi) - \beta[\sin \phi'_2 - \sin \phi_1]$$

$$\frac{v_f}{\omega d} = \beta(\cos \phi_1 - \cos \phi'_2) + \sqrt{2\gamma}$$

Using the sum and difference of the first two relations, we get:

$$\beta[\cos \phi_1 - \cos \phi'_2] = \frac{v_f - v_i}{\omega d}$$

$$\beta[\cos \phi_1 + \cos \phi'_2] = -\frac{v_f + v_i}{\omega d} \cdot \frac{\phi'_2 - \phi_1}{m \pi}$$

$$\beta[\sin \phi_1 + \sin \phi'_2] = 1 - \frac{v_f + v_i}{2 \omega d} \cdot \left[m\pi - \frac{(\phi'_2 - \phi_1)^2}{m \pi} \right]$$

After some transformation, we get:

$$\tan\left(\frac{\phi_1 - \phi'_2}{2}\right) = \frac{1 - \frac{v_f + v_i}{2 \omega d} \cdot \left[m\pi - \frac{(\phi'_2 - \phi_1)^2}{m \pi} \right]}{-\frac{v_f + v_i}{\omega d} \cdot \frac{\phi'_2 - \phi_1}{m \pi}}$$

And:

$$\tan\left(\frac{\phi_1 + \phi'_2}{2}\right) = \frac{-\frac{v_f - v_i}{\omega d}}{1 - \frac{v_f + v_i}{2 \omega d} \cdot \left[m\pi - \frac{(\phi'_2 - \phi_1)^2}{m \pi} \right]}$$

From which we get the phases ϕ_1 and ϕ'_2 and then:

$$\beta = \frac{v_f - v_i}{\omega d [\cos \phi_1 - \cos \phi'_2]} = \frac{v_f - v_i}{-2\omega d \sin\left(\frac{\phi_1 + \phi'_2}{2}\right) \sin\left(\frac{\phi_1 - \phi'_2}{2}\right)}$$

$$\beta = \frac{v_f - v_i}{-2\omega d} \sqrt{1 + \frac{1}{\tan^2\left(\frac{\phi_1 + \phi'_2}{2}\right)}} \sqrt{1 + \frac{1}{\tan^2\left(\frac{\phi_1 - \phi'_2}{2}\right)}}$$

5.2.2 Modes with m odd

If m is odd, we have the 3 following relations:

$$1 = [\sqrt{2\gamma} + \beta \cos \phi_1](\phi'_2 - \phi_1 + m \pi) + \beta[\sin \phi'_2 + \sin \phi_1]$$

$$1 = [-\sqrt{2\gamma} + \beta \cos \phi'_2](\phi'_2 - \phi_1 - m\pi) + \beta[\sin \phi'_2 + \sin \phi_1]$$

$$\frac{v_f}{\omega d} = \beta(\cos \phi_1 + \cos \phi'_2) + \sqrt{2\gamma}$$

After similar computations, we get:

$$\tan\left(\frac{\phi_1 - \phi'_2}{2}\right) = \frac{\frac{v_f + v_i}{\omega d} \cdot \frac{\phi'_2 - \phi_1}{m\pi}}{1 - \frac{v_f + v_i}{2\omega d} \cdot \left[m\pi - \frac{(\phi'_2 - \phi_1)^2}{m\pi}\right]}$$

And:

$$\tan\left(\frac{\phi_1 + \phi'_2}{2}\right) = \frac{1 - \frac{v_f + v_i}{2\omega d} \cdot \left[m\pi - \frac{(\phi'_2 - \phi_1)^2}{m\pi}\right]}{\frac{v_f - v_i}{\omega d}}$$

From which we get the phases ϕ_1 and ϕ'_2 and then:

$$\beta = \frac{v_f - v_i}{\omega d [\cos \phi_1 + \cos \phi'_2]}$$

Remark that if $\phi_1 = \phi'_2$ these last relations are identical to the ones already obtained for the classical mode with $m = 2n - 1$.

5.2.3 Limits of modes

The limits of modes will be given by the same conditions as for classical modes:

$x > 0$; $x < d$; and stability.

Here, both phases ϕ_1 and ϕ_2 must obey the stability condition.

Conditions on $x > 0$ and $x < d$ are obtained by computing the position for all phases between ϕ_1 and ϕ_2 and testing for $x = 0$.

Stability conditions are verified by computing the derivative of the phase after two trajectories:

$$\frac{x(\phi_2)}{d} = [\sqrt{2\gamma} + \beta \cos \phi_1](\phi_2 - \phi_1) - \beta[\sin \phi_2 - \sin \phi_1]$$

$$\frac{d}{d\phi_1} \left[\frac{x(\phi_2)}{d} \right] = -[\sqrt{2\gamma} + \beta \cos \phi_1] - \beta \sin \phi_1 (\phi_2 - \phi_1) + \beta \cos \phi_1$$

$$\frac{d}{d\phi_1} \left[\frac{x(\phi_2)}{d} \right] = -\sqrt{2\gamma} - \beta \sin \phi_1 (\phi_2 - \phi_1)$$

The final speed being v_f , the final phase variation is:

$$d\phi_2 = -\frac{dx}{v_f} \omega = -d \left(\frac{x}{d} \right) \frac{\omega d}{v_f}$$

From which:

$$\frac{d\phi_2}{d\phi_1} = \frac{\omega d}{v_f} [\sqrt{2\gamma} + \beta \sin \phi_1 (\phi_2 - \phi_1)]$$

In the same manner, we have for the return trajectory (replacing β by $-\beta$, ϕ_1 by ϕ_2 and ϕ_2 by $\phi_1 + 2m\pi$):

$$\frac{d\phi_3}{d\phi_2} = \frac{\omega d}{v_f} [\sqrt{2\gamma} - \beta \sin \phi_2 (\phi_1 + 2m\pi - \phi_2)]$$

All over, we have $\frac{d\phi_3}{d\phi_1} = \frac{d\phi_3}{d\phi_2} \frac{d\phi_2}{d\phi_1}$ so that:

$$\frac{d\phi_3}{d\phi_1} = \left(\frac{\omega d}{v_f}\right)^2 [\sqrt{2\gamma} + \beta \sin \phi_1 (\phi_2 - \phi_1)] [\sqrt{2\gamma} + \beta \sin \phi_2 (\phi_2 - \phi_1 - 2m\pi)]$$

The multipactor effect is stable if this product is between -1 and +1.

We obtain the same relation as in the classical case when $\phi_2 = \phi_1 + m\pi$ by remarking that in that case:

$$\frac{v_f}{\omega d} = 2\beta \cos \phi + \frac{v_i}{\omega d}$$

Figure 15 gives the first 4 modes ($m = 1$ to $m = 4$) in the same conditions as figure 6. Remark that classical modes (m odd, $m = 2n - 1$) are larger than in figure 6 and the new mode $m = 2$ follows the classical mode $m = 1$. These two modes are generally measured as the same in experiments that give a minimum power slope of $P = 40 \log(fd)$.

Figure 16 gives the first 4 modes in the same conditions as figure 7, that is considering conditions for $x > 0$ and $x < d$ but not stability condition.

The reason is that we have not considered the generalization to 4, 8, ... trajectories in one cycle so the real envelopes of the modes are somewhere in between those of figure 15 and figure 16.

For $m = 1$, both figures are identical, and the computation of the mode envelope is exact.

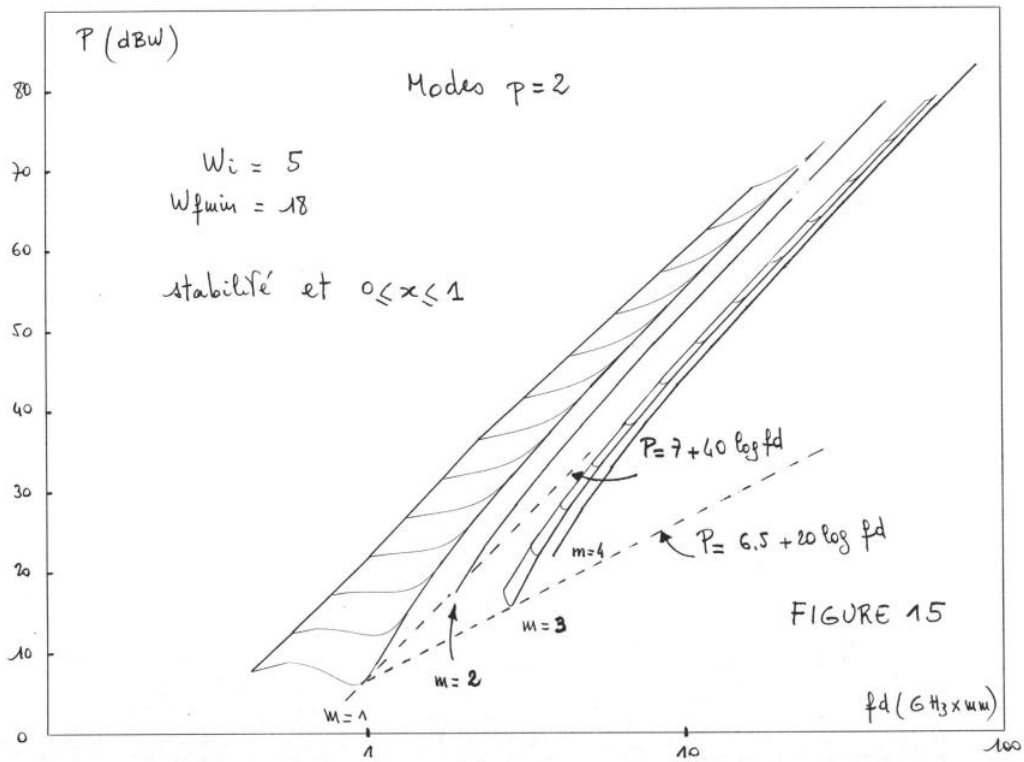
Figure 17 gives an example of mode $m = 2$, $p = 2$ for $fd = 2$ GHz mm.

Stable phases that alternate in the cycle are on two arches of the curve at constant voltage V_0 for a power of $P=18.3$ dB.

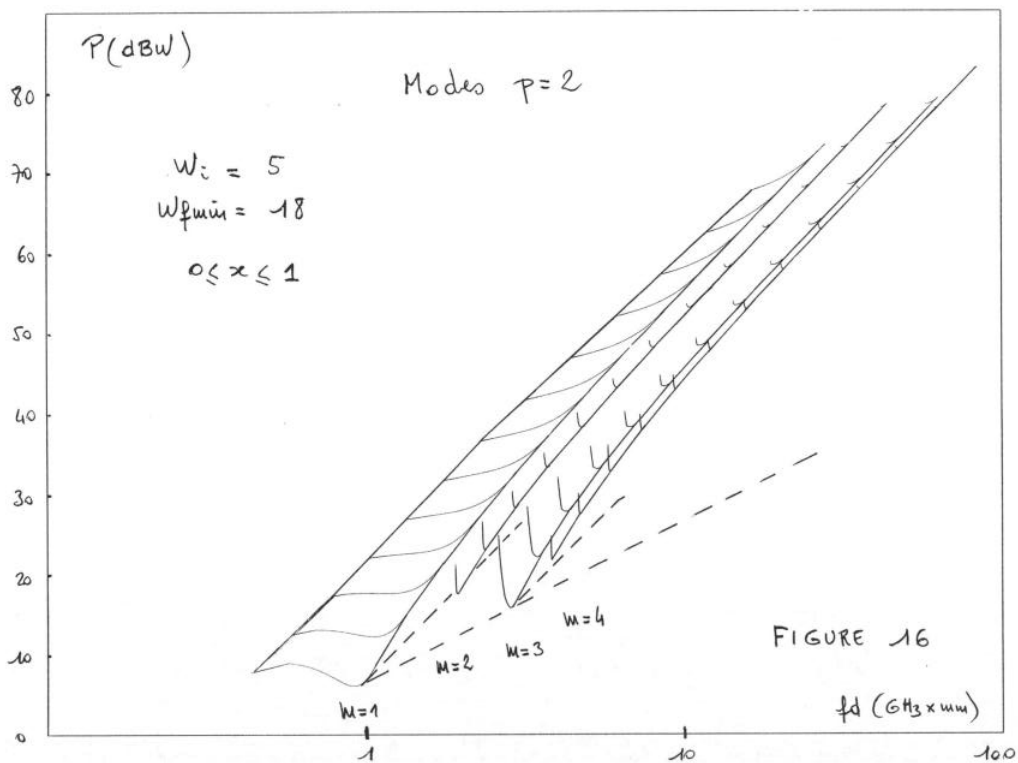
The convergence range is reduced, compared to the classical mode $m = 1$ to about 30° .

Figure 18 gives an example of the widening of the first classical mode $m = 1$, $p = 2$ for $fd = 0.5$ GHz mm.

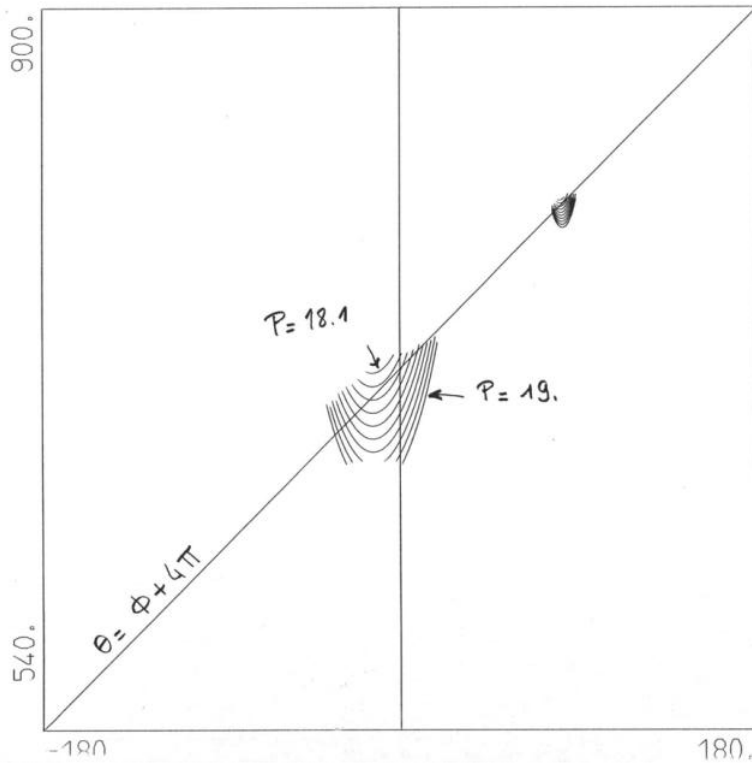
The convergence range is up to 180° for some values of voltage V_0 (power $P=9.5$ dB).



39.



40.



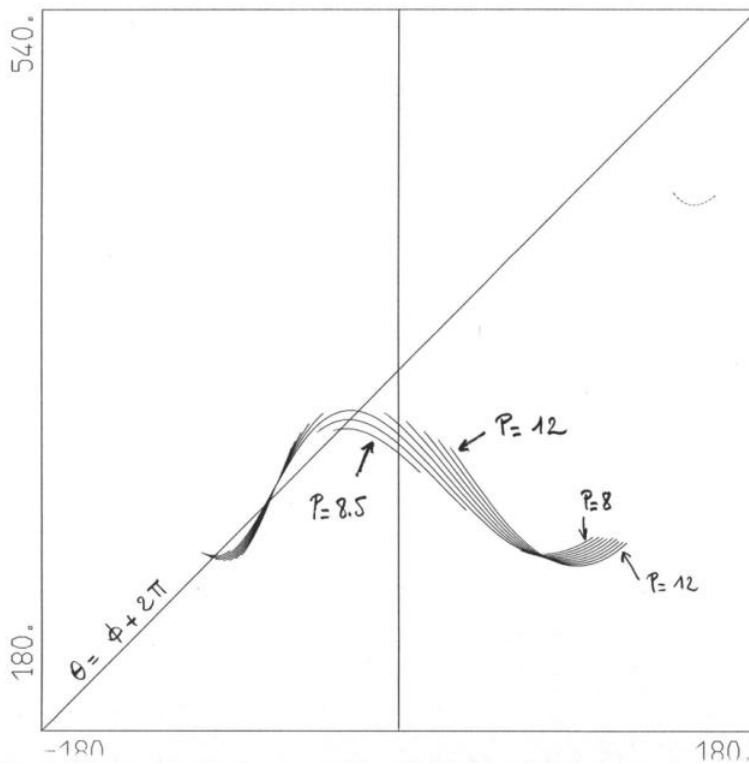
FD = 2.00
 NBTRAJ= 2
 ICYCLE= 1
 ICASE = 2
 PMINDB= 18.10
 PMAXDB= 19.00
 PASDB = .10

MODE: P= 2 trajets
 M= 2
 CYCLE= 4\pi

courbes avec
 v_f ; v_{fmin} seulement

FIGURE 17

42.



FD = .50
 NBTRAJ= 2
 ICYCLE= 1
 ICASE = 2
 PMINDB= 8.00
 PMAXDB= 12.00
 PASDB = .50

MODE: P= 2 trajets
 M= 1

CYCLE = 2\pi

courbes avec
 $v_f > v_{fmin}$ seulement

FIGURE 18

42.

6 Intermittent behavior

Generally, systems with stability and instability zones as a function of a parameter have also zones with intermittent behavior [8].

Starting from a stable zone, if the unstable zone is reached by increasing the value of a parameter (the voltage in our case) the intermittent behavior is obtained when decreasing the value of the same parameter.

Figure 19 shows a $\theta = \theta_f(\phi)$ curve giving the final phase as a function of initial phase for a trajectory. It has been drawn for a value of voltage slightly lower than the one that result in a stable multipactor effect. This curve does not cross the straight line given by $\theta = \phi + \pi$.

Phases $\phi_1, \phi'_2, \phi_3, \phi'_4, \dots$ of the electron trajectory are obtained graphically.

As can be seen, the electron phase delay with respect to electric field increases until it gets to a phase for which there is a discontinuity of the curve $\theta = \theta_f(\phi)$.

The electron can even fall back on the plate which it just left. Its speed is then much smaller than the one obtained at the end of trajectories between opposite plates. The delay is then around 2π .

If that speed is higher than $v_{f \min}$, the phenomenon may go on again. However, the probability to get a stable cycle is low, the movement is chaotic. The number of trajectories in a pseudo-cycle depends on the stability parameter (voltage for us). It can be any integer and not a power of 2. It will vary wildly for small variations of the stability parameter.

If, for any trajectory in the pseudo-cycle, the final speed is less than $v_{f \min}$, the number of secondary electrons will be lower than the number of primary electrons. However, this could be compensated by a greater number of trajectories with final speed higher than $v_{f \min}$. The it is necessary to consider the shape of the electron yield curve versus final energy to determine if the number of electrons increases or decreases during a pseudo-cycle.

Multipactor effect will happen in pseudo-cycles where the average number of electrons increases during a pseudo-cycle.

This definition will give a widening of modes in the direction of lower values of voltage V_0 .

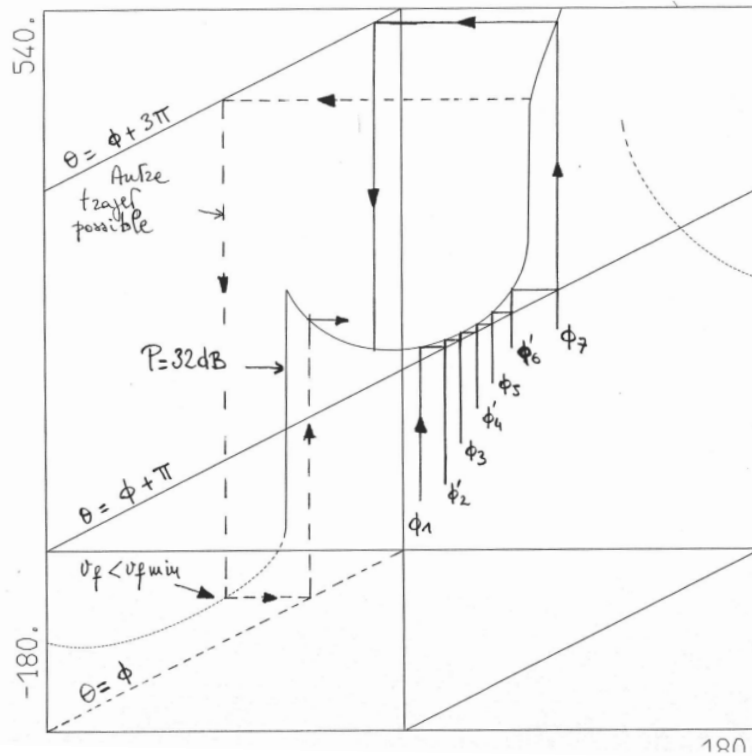
For the first mode, this effect can be observed is the zone between the classical mode ($p=2$; $m=1$) and the new one ($p=2$, $m=2$).

In this zone, we will also find stable modes with values of $p>2$ and values of m between 1 and p but the analytical study has not been generalized to value of $p>2$.

In this zone, values of initial and final phases are distributed between around 0° and 60° .

Final speeds are also distributed with a spike at low final speed and another at high final speed corresponding to phases between 0° and 60° .

The study was done by examining the successive trajectories of one electron.



```

FD = 3.00
NBTRAJ= 1
ICYCLE= -1
ICASE = 4
PMINDB= 32.00
PMAxDB= 32.10
PASDB = 2.00

```

En trait plein :
trajet de $x=0$ à $x=1$

En pointille :
trajet de $x=0$ à $x=0$
(retour sur la plaque de départ)

En rouge : $v_f < v_{f \min}$

FIGURE 19

7 Comparison with experimental results

Most multipactor effect experimental results in microwaves are reported in Hatch and Williams article [3]. They are compared with the authors theory and the one presented here for $eW_{f \min} = 50eV$.

Figure 20 shows the mode obtained with the theory for $eW_{f \min} = 50eV$ together with 3 sets of measurement results with different cleaning conditions:

- Lower curve: after 24 hours in vacuum chamber at $2 \cdot 10^{-3}$ mm Hg
- Middle curve: after half hour discharge at 10^{-4} mm Hg
- Middle curve: after one hour discharge at 10^{-4} mm Hg

Electrodes are aluminum.

Multipactor effect is detected by emitted light.

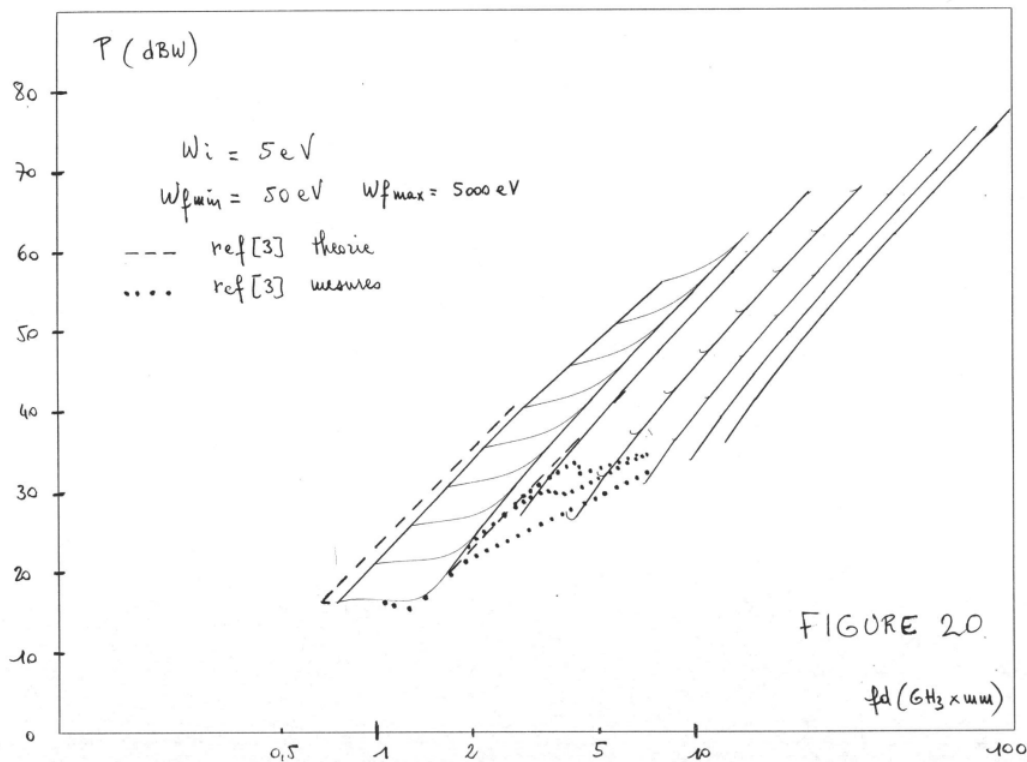
Authors write those parts of the curves with very low multipactor effect could have been unobserved.

The minimum value of fd (cut-off of first mode $m=1$) is 1.05 GHz mm instead of the theoretical value of 0.8 GHz mm. This may come from the detection method.

The value of 50 eV for $eW_{f \min}$ seems to be correct for the first mode but for clean electrodes a value of 70 eV seems to be better for mode $m=3$ ($n=2$) for both theories.

For the less clean electrodes, (24 hours in vacuum chamber at $2 \cdot 10^{-3}$ mm Hg), measurements are near the lower envelope of the classical modes. This not explained by the classical theory but may come from modes with $p>2$ that are between modes $m=1$ and $m=3$ of the classical theory and from intermittent behavior.

Results obtained by other authors are given in [3]. They are near the theory for the first mode.



Hughes study for NASA [9] gives many results concerning metals prepared in engineering conditions (less clean than in the previous study).

All give similar results for the shape of the first mode with a minimum RF voltage between 25 and 35 volts and a cut-off between 0.6 to 0.7 GHz mm.

This corresponds to a final energy of electrons of 18 to 30 eV to result in a unity secondary electron yield.

Even with a detection device more sensitive than in [3], the cut-off is higher than the theoretical values of 0.4 to 0.55 GHz mm.

In addition, the shape is quite different from the theoretical one: nearly vertical cut-off instead of a spike to the lower left (see figure 21).

Remark that the vertical scale range is much smaller than in other figures.

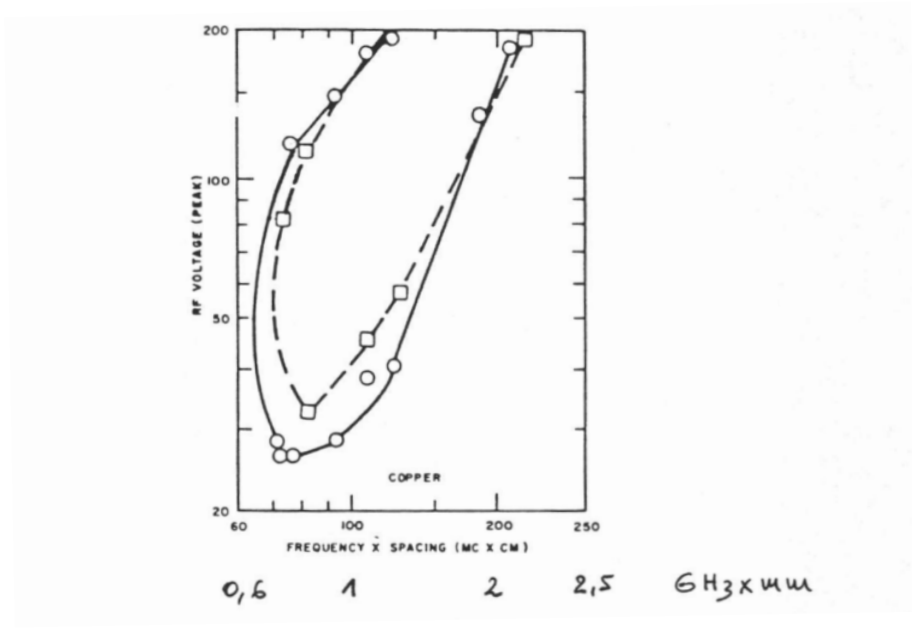


FIGURE 21 - 1er MODE, L'UNE DES COURBES DU RAPPORT HUGHES [9]

The article by H. Tamagawa [10] gives interesting results on the final energy distribution of electrons. He shows that what is considered as the first mode in the classical theory is in fact composed of two parts (see figure 22).

Remark that the vertical scale is linear and not logarithmic as in other figures.

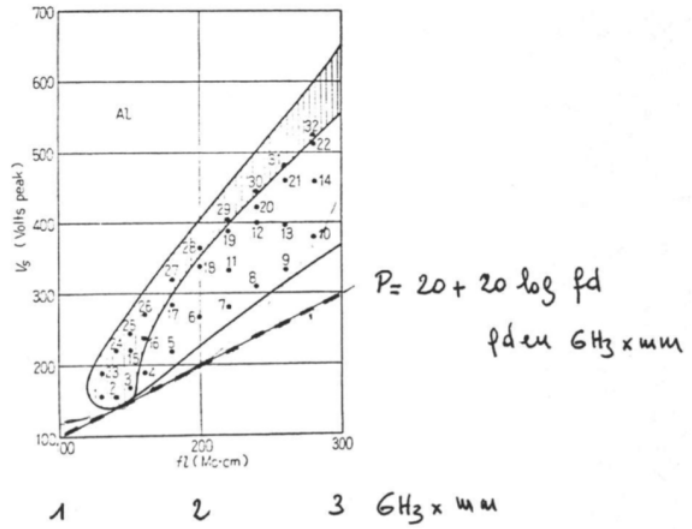


FIGURE 22 - 1er MODE ET SEPARATION EN 2 REGIONS D'APRES TAMAGAWA [10]

In the shaded part (the highest one) the energy distribution has only one spike (coming from the stable mode $m=1, p=2$).

In the unshaded part (the lowest one) the energy distribution has a spike near 0 and another wider one (this is the intermittent behavior of mode $m=1, p=2$ and modes with $p>2$ that are between the first classical modes).

8 Definition of future work

8.1 Study of higher modes

The theory seems to give correctly the first mode but for higher modes a different value must be chosen for $eW_{f \min}$.

Except in some cavities (with high quality factor) used in particle accelerators, modes higher than $n=4$ ($m=7$) were not reported.

Some experimenters suppose that these modes are unstable.

This can be verified by plotting two mode charts with 10% difference for initial speed of secondary electrons (4 eV instead of 5 eV). There is great impact on higher modes; variation of fd product at minimum voltage by: $\frac{d(fd)}{fd} = \frac{dv_i}{v_f + v_i}$

Higher modes having a stable width $\frac{d(fd)}{fd} < 1\%$ there is a clear disjunction between both charts for low final energies $v_f < \text{some } v_i$.

For these higher modes, the convergence range to stable phases is very low (some degrees) whereas the derivative of the final phase with respect to initial speed is high:

$$\delta\phi_2 = \frac{v_i}{v_f} (\phi_2 - \phi_1) \frac{\delta v_i}{v_i}$$

With $(\phi_2 - \phi_1) = m\pi$ in average.

It will be necessary to consider the distribution of secondary electrons initial speeds. An analytical study may be possible by assimilating this distribution to a Gaussian one.

This work is important for prediction of multipactor effect in standard or reduced height waveguides for which the fd product is between 10 and 110.

8.2 Waveguide study

In rectangular waveguides, in the fundamental TE_{10} mode, the electric field E_y is present with two components of magnetic field H_x and H_z .

The H_z magnetic field will push electrons from the median plane where the electric field E_y is maximum, particularly for electrons with an initial phase that is positive.

The H_x magnetic field will infect the trajectory of electrons toward the generator ($z < 0$) et so to decrease the initial phase, and this until it gets out of the convergence range.

However, magnetic forces are much lower than electric forces (100 to 300 times less).

This study could be analytical by considering magnetic forces as a perturbation of electric forces.

8.3 Numerical study

In the case where analytical study would not be feasible and for cases with more complex geometry, it will be necessary to use a numerical computation.

As was shown in chapter 4.5; the electrons initial phase distribution must not be quantified in ranges because this stabilizes unstable modes.

We must start with a certain number of electrons and follow each electron and the secondary electrons generated during many trajectories (50 to 2100) while computing each time the number of secondaries created and choosing a random initial speed, using the energy distribution of secondary electrons. The initial speed direction is also random (cosine law). If the initial speed is not orthogonal to the plate, neither is the final speed. A multiplicative coefficient must be used to compute the number of secondary electrons. Reflected electrons must also be considered.

Article [11] describe such a program applied to particle accelerator cavities.

8.4 Experiments

Experimental results are necessary to define the constants used in the computation (eW_i , eW_{fmin} , ... for different modes) and to study in more details points where the theory does not explain experimental results: cut-off of the fundamental mode, lower envelope of higher modes, influence of cleanliness, ...

This last point is meaningful: plates or devices must be clean (prolonged outgassing, electrical discharge during one hour, hard vacuum) but devices manufactured with space constraints defined by the project and worst case (to be defined).

The vacuum equipment is also meaningful: Hughes report [] shows that a smaller chamber has a more limited own outgassing and that the vacuum pump must be highly efficient: 10^{-9} mm Hg, 125 liters/s. if the tested device is not perfectly outgassed (continuously) the multipactor discharge will stop when the local pressure is too high.

The multipactor effect detection equipment must be sensitive. Electron final energy measurement would be appreciated.

The microwave generator must be able to generate the nominal power for the device plus 6 to 10 dB for standard height waveguides. The test must be carried in continuous wave or at least with pulse duration defined in the project or longer.

In addition to plates, it will be useful to test waveguides with different height or a variable height waveguide (tapper) some irises (for low pass filters) and satellite devices that are available.

9 Conclusion

This technical note presented classically defined multipactor effect.

This effect was studied by choosing a theory (constant initial speed) nearer the physical phenomenon than the one generally used (ratio of final and initial speeds constant).

Through stability and physical limiting conditions, the classical multipactor effects modes have been delimited without using many empirical values as in the simple theory but only 2 (initial speed v_i and minimum final speed v_{fmin} for yield higher than 1).

It was then shown that the classical definition is not sufficient and that modes have an unstable part for higher voltages and an intermittent behavior for lower voltages.

It was also shown that additional modes exist between classical modes.

The analytical study has been done for modes with 2 trajectories per cycle.

Curves giving final phase versus initial phase have been plotted and used to determine the convergence range towards stable phase.

Finally, the theoretical results have been compared with published experimental results and complementary work has been proposed.

10 Additional comments to the English version

After the original French [12] version in 1983, the results were presented in 1984 [13].

An invited talk given at OHD in 1993 [14] presented the results of the program that was implemented following the proposition of this note.

The corresponding papers are available on ResearchGate website.

A large part of the experimental and analytical future work described in the note has been done within collaboration of CNES (Jerome Puech and me)

with Chalmers University of Technology (Prs. Dan Anderson, M. Lisak and J. Rasch; PhD R. Udiljak and U. Jordan),
with the Institute of Applied Physics, RAS, Nizhny Novgorod (Prs. Semenov, E. Rakova and PhD M. Buyanova),
with ONERA in Toulouse (M. Belhadj),
and with industry (TAS, COBHAM).

Many articles by the corresponding authors have been published.
Non-classical multipactor mode were presented as Hybrid Resonant Modes in a different way in a paper with some of these collaborators in 2002 [15].

11 Reference

- [1] P. F. Clancy, "Multipactor Control in Microwave Space Systems", *Microwave Journal*, March 1978, pp. 77-83
- [2] A. J. Hatch and H.B. Williams, "The Secondary Electron Resonance Mechanism of Low-Pressure High-Frequency Gas Breakdown", *Journal of Applied Physics*, 25, 417 (1954)
- [3] A. J. Hatch and H.B. Williams, "Multipacting modes of High Frequency Gaseous Breakdown", *Physical review*, Vol. 112, N° 3, November 1958, pp 681-685
- [4] A. Miller, H. B. Williams, O. Theimer, "Secondary Electron Emission Phase Angle Distribution in High Frequency Multipacting Discharges", *Journal of Applied Physics*, Vol. 34, N° 6, June 1963, pp. 1673-1679
- [5] A. J. Hatch, "Electron Bunching in the Multipacting Mechanism of High Frequency Discharge", *Journal of Applied Physics*, Vol. 32, N° 6, June 1961, pp 1086-1092
- [6] K. Krebs, H. Meerbach, "Die Pendelvervielfachung von Sekundärelektronen", *ANN. Physik*, 15, (1955), pp 189-206
- [7] D. Ofstadter, "Attracteurs étranges", *Pour la Science*, Mars 1982, pp 16-25 and references p 134
- [8] V. Croquette, "Déterminisme et chaos", *Pour la Science*, Décembre 1982, pp 62-77 and references p 134
- [9] Hughes Aircraft Company, "The Study of Multipactor Breakdown in Space Electronic Systems", NASA C448
- [10] H. Tamagawa, "On the Mechanism of the High Frequency Vacuum Discharge" *ETJ of Japan*, Vol 3, June 1957, pp 42-46
- [11] I. Ben Zvi, J. F. Crawford, J. Turneaure, "Electron Multipaction in Cavities", *IEEE Trans. Nuclear Sciences*, Vol NS 20, N° 3, June 1973, pp 54-58
- [12] J. Sombrin, "Effet Multipactor", *CNES Note 83/DRT/TIT/HY/119/T*, 10 octobre 1983
- [13] J. Sombrin, "Effet Multipactor : extension de la definition à une double infinie de modes – Étude analytique et par simulation", *Journées Nationales Microondes*, 1984
- [14] J. Sombrin, "Claquage Hyperfréquence et effet multipactor dans les satellites", invited talk at *OHD 93*, Paris
- [15] A. Kryazhev, M. Buyanova, V. Semenov, D. Anderson, M. Lisak, J. Puech, L. Lapiere and J. Sombrin, "Hybrid resonant modes of two-sided multipactor and transition to the polyphase regime", *Physics of Plasmas*, Vol 9, N° 11, November 2002, pp 4736-4743